



# CHORUS

This is the accepted manuscript made available via CHORUS. The article has been published as:

## Marginal stability and traveling fronts in two-phase mixtures

N. G. Cogan, Matthew Donahue, and Mark Whidden

Phys. Rev. E **86**, 056204 — Published 5 November 2012

DOI: [10.1103/PhysRevE.86.056204](https://doi.org/10.1103/PhysRevE.86.056204)

# Marginal Stability and Traveling Fronts in Two-Phase Mixtures

N. G. Cogan,<sup>1</sup> Matthew Donahue,<sup>1</sup> and Mark Whidden<sup>1</sup>

<sup>1</sup>*Department of Mathematics, Florida State University, Tallahassee, FL 32306, USA*

Mixtures of materials that move relative to each other arise in a variety of applications, especially in biophysical problems where the mixture consists of materials with different material properties. The variety of applications leads to a bewildering array of multiphase models, each with slightly different behaviors and interpretations, depending on the application. Some of the behaviors include phase separation, traveling waves and linear instabilities. Because of the variability of the predicted behaviors, there has been considerable attention paid to minimal models to determine the fundamental solutions, bifurcations and instabilities. In this manuscript, we describe a new solution for the simplest two-phase system where both phases are dominated by viscous forces, one phase response to osmotic forces and the phases interact through a drag term. The system develops a traveling front separating an unstable, uniform solution from a patterned, phase separated solution. We seek the velocity of the traveling front and show that, for large diffusion, marginal stability gives a simple and accurate prediction for the velocity. For smaller diffusion constants, the front is ‘pushed’, and the linear prediction fails.

PACS numbers: 89.75.Kd

## INTRODUCTION

Multiphase models were initially developed to describe the dynamics of heterogeneous mixtures of materials without focusing on the microscopic interactions, instead focusing on macroscopic interactions. Multiphase models avoid describing the material using a single constitutive law as other models such as Oldroyd-B do. Primarily this is because multiphase models focus on applications where there are clearly more than one material and the relative motion and distribution of the materials is of primary interest. One example is the dynamic swelling of poly-electrolyte gels which are formed from networked polymer that is hydrated by water [1]. Submerging a region of gel within a bath of water causes the gel to undergo deformations as the gel absorbs or expels water due to the osmotic nature of the polymer network. In addition, multiphase models are increasingly used to describe biological processes. They have been used to describe the dynamics of biofilm growth and development, tumor aggregation, and cell blebbing [2].

With the growing diversity of applications where multiphase models are employed, there is subsequent focus on understanding the dynamics of these models. However, these models are extremely flexible and exhibit a range of behaviors. In addition to deformations that occur because of changes in the external state (such as osmotic swelling described above), multiphase models have been used couple fluid motion to the deformation of bacterial communities termed biofilms. Since the biofilms are mixtures of water and polymer, multiphase models join the fluid and the biofilm regions smoothly, similar to the regularization of phase-field models [3, 4]. This is a computational advantage of the modeling framework that exploits the averaging of the multiphase models. It is also well known that multiphase models that include osmotic

forces will phase-separate [3–5]. Since the osmotic forces drop out if there is no network, or the network is in its “preferred” density, uniform distributions are generically unstable to perturbations [5, 6].

Recently, there have been studies that focus on traveling wave behavior of similar multiphase models [7–9]. In [7] a simplified model is introduced and the authors describe how initial conditions and perturbations can select for the velocity and direction of the traveling wave and further relate this to cell crawling. In one dimension and after long times, the traveling wave shape and speed can be related to the parameters as in [9]. In [8] the authors use the model from [3] and analyze the spreading of an initially aggregate under suitable limiting parameter values. The wave speed of a solution that arises from a departure from the uniform solution is obtained numerically and related to experimental observations. Finally, the two-phase model of biofilm growth introduced in [3] and used in [8] exhibits traveling fronts after long time evolution [9]. We note that in last two applications there is a feedback between production of one phase (the network phase) and subsequent motion driven by gradients in the osmotic pressure while the first system is driven by asymmetries in the perturbations. It has been argued that the multiphase framework is a natural description of redistribution of mass for a wide array of biological processes [2] and can drive systems to reinforce some wavelength perturbations, or drive domain motion.

In this manuscript, we describe a different mode of redistribution that, like the ones described above, is initiated by a departure from an equilibria. However, this solution is not driven by production of one phase, nor does it follow from classical linear instability arguments. Instead, we note that *localized* perturbations lead to a traveling front that separates a patterned region from a uniform region. The aim is to determine the speed of the

propagating front. We note that this solution may play a role in the development and spreading of biofilm patterns that are observed in microfluidic chambers where the bacterium *Xylella fastidiosa* (the causative agent of Pierce's Disease) is introduced. Over the course of seven days, a clear pattern is seen to travel throughout the domain.

We argue here that this behavior is built into the simplest multiphase model and that the motion of the front can be understood using marginal stability analysis. The model that we use is a simplification of the model described in [3] and also described in [10]. In particular, here we do not try and relate the physics of the forces to particular biological or biophysical processes. Instead we consider a stripped-down, heuristic model that contains the mechanisms that ensure reasonable interactions between the phases (through interphase friction), within each phase (viscous forces), forces that induce phase separation (osmotic forces) and forces that arise from incompressibility (hydrostatic pressures). This is a different approach than in [3] that describes a particular biological process. In a later study, we will extend this model to the particular case of biofilm mechanics, but the goal here is to focus on deriving theory to understand the spread of patterns in a multiphase model.

There are several other studies that also focus on the spread of phase separation. The velocity of phase separation fronts was determined analytically and/or numerically in [11–13] for diffusive dynamics governed by gradient-flow dynamics; however, gradient-flow is much simpler than the situation considered here that includes the momentum of the phases. Rather than a front of polymerization, we are focusing on situations that involve mass redistribution and momentum cannot be neglected. In [14, 15] the momentum is considered and numerical methods are used to study the advancing front and one of the novel aspects of this manuscript is the application of marginal stability analysis that, while an approximation, is more general than purely numerical observations and much simpler than other analytic methods.

## MODEL DEVELOPMENT

We assume that a region of space is occupied by a mixture of two phases that occupy volumes,  $\theta_n$  and  $\theta_f$  (referring to the polymer network and fluid volume fractions, respectively). The entire space is occupied by either  $\theta_n$ ,  $\theta_f$ , or a mixture of the two. This implies a *saturation* condition  $\theta_n + \theta_f = 1$ , that excludes any other volume. Each of the components move with their own velocity,  $\mathbf{u}_n$  and  $\mathbf{u}_f$ . The model consists of statements of conservation of volume and momentum for each of the phases. We pose the model in one-dimension, but the model is easily applied to multiple dimensions.

We include diffusion in the volume fraction, so that

the time rate of change of the volumes is balanced by advection and diffusion. The diffusion coefficients are assumed to be equal, for simplicity and this is discussed further below. Conservation of volumes (or masses if the densities of the phases are equal) are:

$$\frac{\partial \theta_n}{\partial t} + \frac{\partial(\theta_n \mathbf{u}_n)}{\partial x} = \kappa \frac{\partial^2 \theta_n}{\partial x^2}, \quad (1)$$

$$\frac{\partial \theta_f}{\partial t} + \frac{\partial(\theta_f \mathbf{u}_f)}{\partial x} = \kappa \frac{\partial^2 \theta_f}{\partial x^2}. \quad (2)$$

Conservation of momentum for each phase and the saturation condition yield the final governing equations. In typical multiphase models, the viscous forces dominate so that each phase is in force balance and inertial terms are neglected. Forces from the viscosity of each phase are denoted  $\mathbf{F}_i^{viscous} = \mu_i \frac{\partial(\theta_i \frac{\partial \mathbf{u}_i}{\partial x})}{\partial x}$  (implying that each phase is a viscous fluid). The phases also interact through friction which is incorporated as a drag force that is proportional to the difference in the phase velocities,  $\mathbf{F}_n^{drag} = \beta \theta_n \theta_s (\mathbf{u}_n - \mathbf{u}_f)$  and the equal and opposite force for the fluid:  $\mathbf{F}_f^{drag} = \beta \theta_n \theta_s (\mathbf{u}_f - \mathbf{u}_n)$ . Notice that frictional interaction disappears if neither of the phases is present ( $\theta_i = 0$ , for  $i = n, f$ ) or if there is no velocity difference. This is the simplest interaction between the phases that can be considered. Gradients in hydrostatic pressure,  $P$ , that arise to enforce incompressibility also induce forces on both phases and are denoted  $\mathbf{F}_i^{pressure} = \theta_i \frac{\partial P}{\partial x}$  (just as in standard fluid equations). Finally, since the polymer network is composed of chemically active polymers, there is an additional osmotic force that acts on the network phase. We use a simplified Flory-Huggins theory to relate this force algebraically to the network volume fraction. We denote this force  $\mathbf{F}_n^{osmotic} = \gamma \frac{\partial \Psi \theta_n}{\partial x}$ , where  $\Psi(\theta_n) = \theta_n^2 (\theta_n - \hat{\theta})$  denotes the osmotic pressure. The specific term chosen here was derived in [3] as an approximation to the standard mixing free energy. In the previous case, the parameters were fixed by comparisons with biofilm experiments. Here the motivation is different; we are focusing on a simple multiphase model that exhibits phase separation and this form of the osmotic pressure has been shown to be a minimal requirement [16].

We note in passing that some authors [5] argue that the osmotic force acts on both phases, but it is easily shown that by redefining the hydrostatic pressure as the sum of hydrostatic pressure and  $\mathbf{F}_f^{osmotic} = 0$ . This rescaling gives a statement that is equivalent to our formulation, therefore we set  $\mathbf{F}_f^{osmotic} = 0$ .

Conservation of momentum for the two phases, described as a force balance is then  $\mathbf{F}_i^{viscous} + \mathbf{F}_i^{drag} + \mathbf{F}_i^{pressure} + \mathbf{F}_i^{osmotic} = 0$  for  $i = n, f$ . This gives the two momentum equations:

$$\frac{\partial(\mu_n \theta_n \frac{\partial \mathbf{u}_n}{\partial x})}{\partial x} - \beta \theta_n \theta_f (\mathbf{u}_n - \mathbf{u}_f)$$

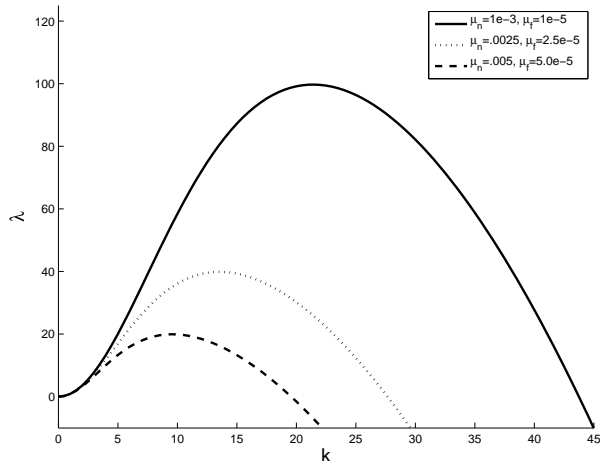


FIG. 1: Dispersion curves for varying viscosities. We vary the viscosities,  $\mu_n$  and  $\mu_f$  while keeping the ratio  $\frac{\mu_n}{\mu_f} = 100$ .

$$-\theta_n \frac{\partial P}{\partial x} - \frac{\partial \Psi(\theta_n)}{\partial x} = 0, \quad (3)$$

$$\frac{\partial(\mu_f \theta_f \frac{\partial \mathbf{u}_f}{\partial x})}{\partial x} - \beta \theta_n \theta_f (\mathbf{u}_f - \mathbf{u}_s) - \theta_f \frac{\partial P}{\partial x} = 0. \quad (4)$$

### LINEAR ANALYSIS: DISPERSION CURVES AND MARGINAL STABILITY

It is quite easy to see that any uniform distribution of phases ( $\theta_n = \theta_n^0$  and  $\theta_f = \theta_f^0$ , both constant in space) is a solution with constant pressure as long as  $\mathbf{u}_n^0 = \mathbf{u}_f^0$ . Throughout, we assume that the uniform velocities are both zero. It is likewise easy to determine the linear stability of these solutions to perturbations in space. Assuming that  $\theta_n = \theta_n^0 + \epsilon \theta_n^1 e^{-i\lambda t + ikx}$ ,  $\theta_f = \theta_f^0 + \epsilon \theta_f^1 e^{-i\lambda t + ikx}$ ,  $\mathbf{u}_n = \epsilon \mathbf{u}_n^1 e^{-i\lambda t + ikx}$  and  $\mathbf{u}_f = \epsilon \mathbf{u}_f^1 e^{-i\lambda t + ikx}$  and substituting into Equations 1, 2, 3 and 4 we obtain a linear system of equations of the form  $\mathbf{A}\mathbf{v} = \mathbf{0}$  for the amplitude of the perturbations,  $\mathbf{v} = (\theta_n^1, \theta_f^1, \mathbf{u}_n^1, \mathbf{u}_f^1)$ . Since we seek non-trivial perturbations the determinant of  $\mathbf{A}$  must be zero. This requirement yields a *dispersion* relation between the growth rate,  $\lambda$ , and the wave number,  $k$ , of the perturbation. The dispersion relation carries information about the growth/decay of perturbations – by solving the relationship for  $\lambda(k)$ , we see that perturbations may grow if  $\text{Im}(\lambda) > 0$ , while others do not. The dispersion relation is relatively complicated and depends on the parameters of the model so we do not write it explicitly, but Figure 1 shows the dispersion curve for a variety of parameters. Note that typically small wave numbers (e.g. long wavelength) perturbations are unstable, while all sufficiently high frequency perturbations decay.

Classical linear stability argues that spatial patterns may arise from global perturbations from an equilibrium

state; however, in the time course many experiments, it is clear that the pattern does not appear throughout the entire domain. In fact, the uniform solution (with no material) is invaded by a patterned region. In the simple two-phase model described here, Figure 2 compares the time-course for the dynamics that start with the same initial state. The first panel shows the results with a random perturbation throughout the domain, while the second panel shows the results of a localized perturbation. Interestingly, for a local perturbation, we see an invasion front where the patterned solution moves into the uniform region at a more-or-less constant rate.

Even though the simple model does not include any biological mechanisms, we still see a traveling wave of sorts. We can then try and determine the wave speed. We show that the marginal stability hypothesis give quite accurate predictions of the wave speed for a range of parameters. Marginal stability is based on early work by Dee and Langer [17] who proposed a very simple mechanism to explain how patterns can develop in nonlinear systems. They argue that the speed of propagation is the speed at which the system is neither growing nor decaying as one moves with the disturbance. Moreover, this speed can be determined directly from the dispersion curve,  $\lambda(k)$  by solving  $\frac{d\lambda}{dk} - v^* = 0$ ;  $\text{Im}(\lambda(k^*) - v^* k^*) = 0$ , for the wave speed,  $v^*$  and mode  $k^*$ . This works for several models where the wave-speed can be determined analytically and is a bit surprising, since the underlying models are nonlinear and rely only on the dispersion curve that comes from the linearization. This idea has been explored more fully [18] and, as long as the model is not 'too' nonlinear, the basic idea is quite correct. The reason the linear theory is predictive has to do with the formal linearization of the patterning solution around the leading front. As long as the nonlinearities do not draw in too much information, the local analysis dominates. When this is true the front is referred to as a *pulled* front. Otherwise, when the linear theory does not predict the wave-speed, the front is termed *pushed* [19, 20].

The simple, linear marginal stability analysis rests on the assumption that the spreading velocity (the speed of the front between the uniform, unstable state and the stable patterned regions) that is generated by spatially isolated perturbations can be found by linearizing the equations about the unstable state. This is quite unexpected, since only the linear terms are included. There are various arguments that can be used to generate the simple hypothesis that the wave speed can be found from the dispersion curve,  $\lambda(k)$  by solving the coupled system:

$$\frac{d\lambda(k^*)}{dk} = \frac{\text{Im}(\lambda(k^*))}{\text{Im}(k^*)}$$

$$v^* = \frac{d\lambda(k^*)}{dk}$$

for the speed  $v^*$  and mode  $k^*$ . This can be derived from heuristic arguments (that the speed and mode are found

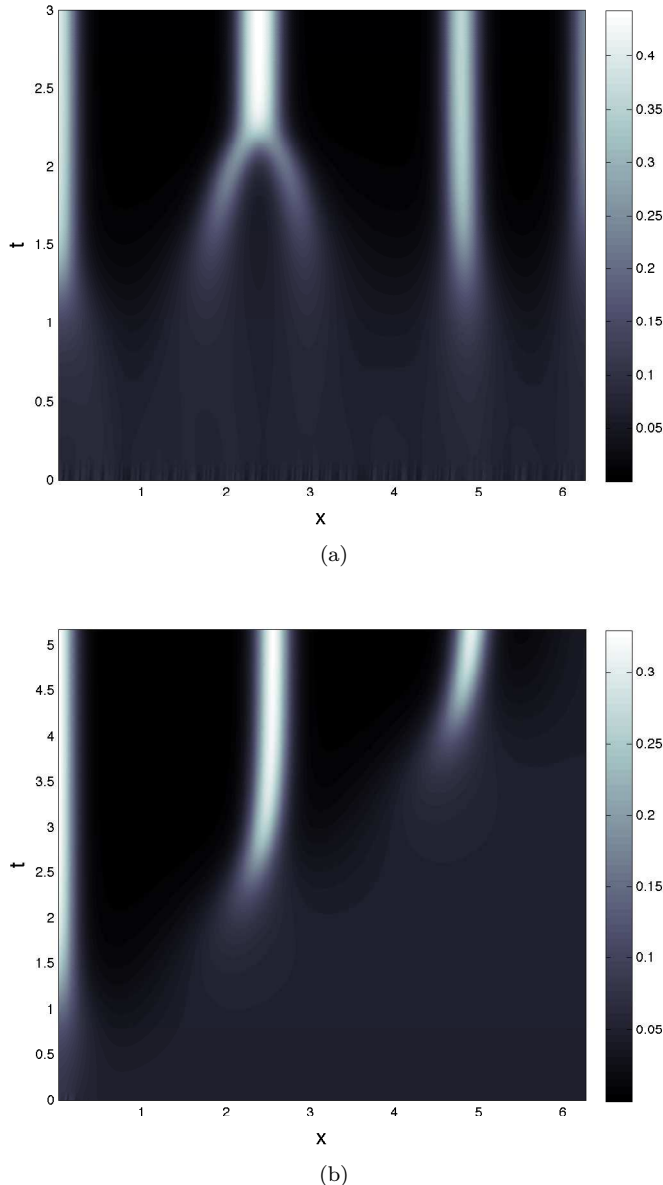


FIG. 2: Panel (a) shows the phase separation dynamics from a perturbation that is applied to the entire domain. Panel (b) show the dynamics when the perturbation is restricted to a small region near  $x = 0$ . We see an invasion front of pattern that moves into the, initially, un-patterned region.

from the *marginal stability* of the linear theory, i.e. where the dispersion curve is zero), from more formal arguments [18] or from the theory of pinch-point [18].

Using this, and the fact that we have a dispersion curve, we can compare predicted speeds with numerical simulations to see that the predictions are quite accurate for a range of parameters. First, we should discuss the numerical methods that are used for the simulations, which is based on the scheme given in [9]. For a given

initial distribution of network and fluid volume fractions, the network and fluid velocities and pressure are solved using a multigrid method, which can also be used as a right preconditioner for Krylov subspace methods to enhance robustness. The multigrid method uses standard prolongation and restriction operators and red-black box (or Vanka) relaxation for the smoother. To step forward in time, we use explicit first-order upwinding for advection and implicit Euler for diffusion. The system is discretized using second-order finite differences on a MAC grid. There are ample details in the implementation that are discussed in [9] that require substantial sophistication in the choice of preconditioning and multigrid cycling. We note that the images in Figure 3 were found using this scheme and our implementation is in agreement with those published in [9] although the comparisons are not shown here.

We are now in a position to use the marginal stability theory in conjunction with the numerical methods to estimate the front propagation speed. We keep most parameters fixed and allow the viscosities to vary (with constant ratio). Specific parameters, in nondimensional form, are  $\beta = .2$ ,  $\Psi(\theta_n) = \gamma\theta_n^2(\theta_n - \hat{\theta})$  with  $\gamma = 5$ ,  $\kappa = 0.1$  and  $\hat{\theta} = 0.5$ . As we change the viscosities between  $\mu_n = [0.0005, 0.005, 0.05]$  and  $\mu_f = [0.000005, 0.00005, 0.0005]$  (note that the network is assumed to be 100 times as viscous as the fluid).

## CONCLUSIONS

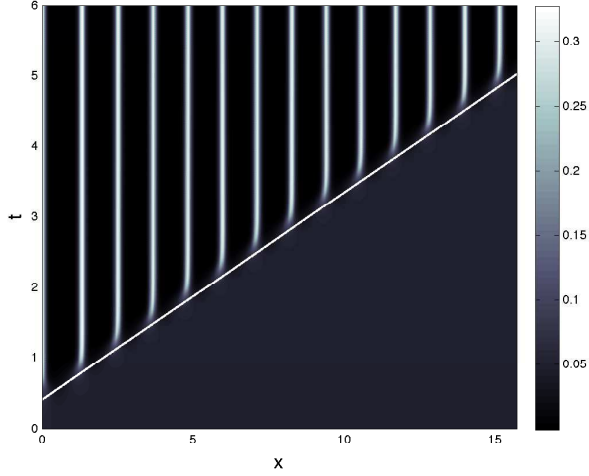
There are several things to notice about these results. First, there is a correspondence between the maximally unstable modes (the maximum of the dispersion curve) and the corresponding patterning frequency. The bottom panel has the highest maximally unstable mode and correspondingly higher frequency pattern. Likewise the speed at which the pattern appears correlates well with the magnitude of the positive regions of  $\lambda$ .

Even though these results are quite promising, they are only valid when the front is 'pulled', rather than 'pushed' by the nonlinearities. This can be seen by decreasing the diffusion coefficient which makes the nonlinear terms contribute more to the behavior. When we set  $\kappa = 0.001$ , we find that the velocity predicted by the marginal stability calculation fails (see Figure 4). As is typical for pushed fronts, the propagating front moves faster than the speed predicted by the linear theory. The analysis of the pushed front parameter regime is beyond the scope of this paper and requires much more delicate reasoning.

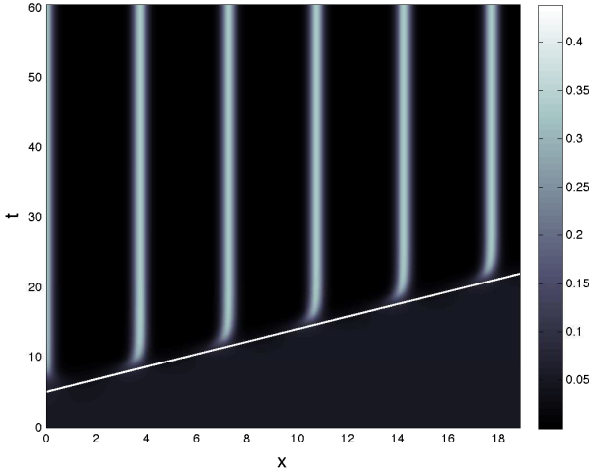
The purpose of this manuscript is to introduce a new class of solutions for multiphase systems. These solutions are characterized by a patterned region that moves into a uniform region. To our knowledge these solutions have not been discussed previously; however they may play an important role in physical or biological systems

where the interactions between components of the system lead to propagating patterns. Our motivating physical system is that of bacterial biofilms that form within plant xylem referred to as Pierces' Disease. *X. fastidiosa* biofilms grown in artificial xylem (microfluidic chambers) show an apparent spreading pattern that may be linked to the spread of the disease within plant xylem. It is important to be able to estimate the time it takes for the biofilm to spread— which is quite difficult to do *in situ* since the spreading rates correlates with disease progression. The analysis discussed above, while applied to a very simple model, gives a direction to push the analysis for a biologically relevant model.

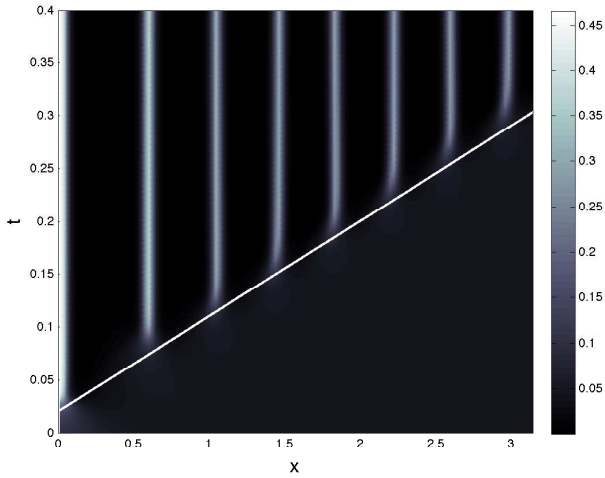
- 
- [1] Charles W. Wolgemuth, Alexander Mogilner, and George Oster. The hydration dynamics of polyelectrolyte gels with applications to cell motility and drug delivery. *European Biophysics Journal*, 33:146–158, 2004. 10.1007/s00249-003-0344-5.
- [2] N. G. Cogan and R. D. Guy. Multiphase flow models of biogels from crawling cells to bacterial biofilms. *HFSP J*, 4:11–25, 2010.
- [3] N. G. Cogan and James P. Keener. The role of the biofilm matrix in structural development. *Mathematical Medicine and Biology*, 21(2):147–166, 2004.
- [4] I. Klapper and J. Dockery. Role of cohesion in the material description of biofilms. *Phys. Rev. E*, 74:031902, Sep 2006.
- [5] James P. Keener, Sarthok Sircar, and Aaron L. Fogelson. Kinetics of swelling gels. *SIAM J. APPL. MATH.*, 71(3):854875, 2005.
- [6] N. G. Cogan and James P. Keener. Channel formation in gels. *SIAM J. APPL. MATH.*, 65(6):1839–1854, 2005.
- [7] L. S. Kimpton, J. P. Whiteley, S. L. Waters, J. R. King, and J. M. Oliver. Multiple travelling-wave solutions in a minimal model for cell motility. *Mathematical Medicine and Biology*, 2012.
- [8] Agnese Seminara, Thomas E. Angelini, James N. Wilking, Hera Vlamakis, Senan Ebrahim, Roberto Kolter, David A. Weitz, and Michael P. Brenner. Osmotic spreading of bacillus subtilis biofilms driven by an extracellular matrix. *Proceedings of the National Academy of Sciences*, 109(4):1116–1121, 2012.
- [9] H. F. Winstanley, M. Chapwanya, M. J. McGuinness, and A. C. Fowler. A polymersolvent model of biofilm growth. *Proceedings of the Royal Society A: Mathematical, Physical and Engineering Science*, 2010.
- [10] G. Wright, R. Guy, and A. Fogelson. An efficient and robust method for simulating two-phase gel dynamics. *SIAM Journal on Scientific Computing*, 30(5):2535–2565, 2008.
- [11] E. M. Foard and A. J. Wagner. Survey of morphologies formed in the wake of an enslaved phase-separation front in two dimensions. *Phys. Rev. E*, 85:011501, Jan 2012.
- [12] E. M. Foard and A. J. Wagner. Enslaved phase-separation fronts and lieegang pattern formation. *Commun. Comput. Phys*, 9:1081–1093, 2010.
- [13] E. M. Foard and A. J. Wagner. Enslaved phase-separation fronts in one-dimensional binary mixtures. *Phys. Rev. E*, 79:056710, 2009.
- [14] A. Tiribocchi, N. Stella, G. Gonnella, and A. Lamura. Hybrid lattice boltzmann model for binary fluid mixtures. *Phys. Rev. E*, 80:026701, Aug 2009.
- [15] G. Gonnella, A. Lamura, A. Piscitelli and A. Tiribocchi. Phase separation of binary fluids with dynamic temperature. *Phys. Rev. E*, 82:046302, Oct 2010.
- [16] NG Cogan and J.P. Keener. Channel formation in gels. *SIAM Journal on Applied Mathematics*, pages 1839–1854, 2005.
- [17] G. Dee and J. S. Langer. Propagating pattern selection. *Phys. Rev. Lett.*, 50:383–386, Feb 1983.
- [18] Wim van Saarloos. Front propagation into unstable states. *Physics Reports*, 386(26):29 – 222, 2003.
- [19] Wim van Saarloos. Front propagation into unstable states: Marginal stability as a dynamical mechanism for velocity selection. *Phys. Rev. A*, 37:211–229, Jan 1988.
- [20] Wim van Saarloos. Front propagation into unstable states. ii. linear versus nonlinear marginal stability and rate of convergence. *Phys. Rev. A*, 39:6367–6390, Jun 1989.



(a)



(b)



(c)

FIG. 3: Comparisons for the marginal velocity obtained using linear theory (solid line) with the patterning obtained by the numerical solutions. Figure 1 shows the corresponding dispersion curves. Panel (a):  $\mu_n = 0.05$ ,  $\mu_f = 0.0005$ . The predicted velocity is 1.1, the reciprocal of the slope of the white line. Panel (b):  $\mu_n = 0.005$ ,  $\mu_f = 0.00005$ . The predicted velocity is 3.5. Panel (c):  $\mu_n = 0.0005$ ,  $\mu_f = 0.000005$ . The predicted velocity is 11.1.

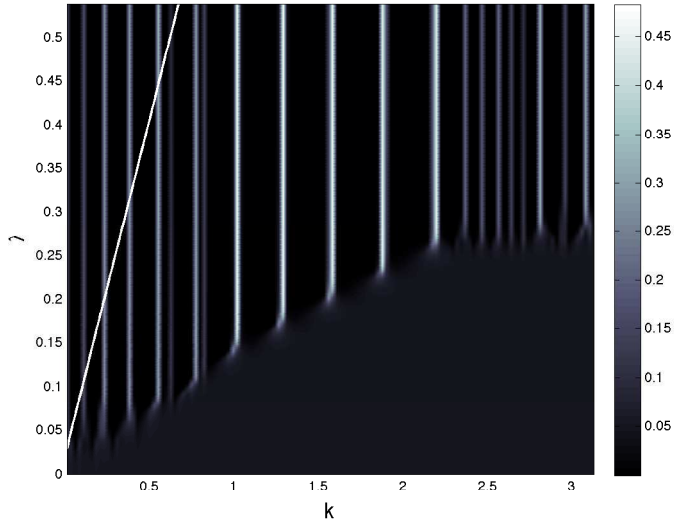


FIG. 4: As the diffusion coefficient,  $\kappa$  is decreased to 0.001, we see that the marginal stability prediction is very inaccurate (shown in white). Moreover, the front is not moving at a constant rate. There are obvious alterations in the width and spacings of the patterns. Therefore, even if the predicted slope was accurate, which it clearly is not, simple linear front velocity is not an accurate description of the pushed front.